Alexey Mikaberidze, Christopher C. Mundt, and Sebastian Bonhoeffer. Invasiveness of plant pathogens depends on the spatial scale of host distribution. *Ecological Applications* .

Appendix S1: Mathematical methods and estimation techniques

S1.1: Linear stability analysis of the disease-free equilibrium

We linearize the model Eqs. (1)-(3) in the vicinity of the disease-free fixed point $H(x,y,t) = K$, $I(x,y,t) = 0$, $R(x,y,t) = 0$ and obtain the following equations for the small deviations from this fixed point $\xi(x,y,t)$ and $I(x,y,t)$:

$$\frac{\partial \xi(x,y,t)}{\partial t} = -r_H \xi(x,y,t) - \beta K \int \kappa(x,y,u,v) I(u,v,t) du\, dv, \tag{S.1}$$

$$\frac{\partial I(x,y,t)}{\partial t} = \beta K \int \kappa(x,y,u,v) I(u,v,t) du\, dv - \mu I(x,y,t). \tag{S.2}$$

The disease-free fixed point becomes unstable if the small deviation $I(x,\, y,\, t)$ grows over time. To check this, we substitute $I(x,\, y,\, t) = w(x,\, y) e^{\lambda t}$ in Eq. S.2. Then, the stability of the disease-free fixed point is determined by solving eigenvalue problem

$$\frac{\beta K}{\mu} \int_0^{d_x} du \int_0^{d_y} dv\, \kappa(r) w(u,v) = \sigma w(x,y), \tag{S.3}$$

where $\sigma = 1 + \lambda/\mu$. The eigenvalue problem here consists in finding the values of λ_j and functions $w(x,y)$ satisfying the relationship (A.3). The disease-free fixed point is unstable if at least one of λ_j has a positive real part. Eq. 6 is the homogeneous Fredholm equation of the second kind and can be solved numerically using the Nystrom method (Press et al., 1992). The dominant eigenvalue σ_d determines the basic reproductive number, i. e. $R_0 = \sigma_d$. Note that the eigenvalue problem Eq. S.3 also determines the stability properties of the corresponding integro-difference system of equations in discrete time.

S1.2 Approximation for the basic reproductive number

Approximate expression for the basic reproductive number for the model Eqs. (1)-(2) can be found by applying its intuitive definition "the average number of secondary cases of infection generated by one primary case in a susceptible host population" (Anderson and May, 1986) with the averaging performed over the spatial coordinates. This leads to the expression:

$$R_{0\mathrm{c}}(x_0, y_0) = \frac{\beta K}{\mu} \int_0^{d_x} dx \int_0^{d_y} dy\, \kappa(x,y,x_0,y_0). \tag{S.4}$$

Here, the basic reproductive number depends on the position x_0, y_0 of the initial inoculum. The basic reproductive number in Eq. S.4 does not yield the invasion threshold at $R_{0\mathrm{c}}(x_0, y_0) = 1$ (Diekmann et al., 1990). However it may serve as a useful approximate expression, since the calculation

according to Eq. S.4 is often much simpler than the solution of the eigenvalue problem Eq. S.3. In order to determine how good this approximation is, we obtain an explicit expression for $R_{0c}(x_0, y_0)$

$$R_{0c}(x_0, y_0) = \frac{\beta K}{4\mu}\left[\mathrm{erf}\left(\frac{d_x - x_0}{\sqrt{2}d}\right) + \mathrm{erf}\left(\frac{x_0}{\sqrt{2}d}\right)\right]\left[\mathrm{erf}\left(\frac{d_y - y_0}{\sqrt{2}d}\right) + \mathrm{erf}\left(\frac{y_0}{\sqrt{2}d}\right)\right], \quad \text{(S.5)}$$

where we substituted $\kappa(r)$ in Eq. S.4 with the Gaussian dispersal kernel

$$\kappa_G(r) = \kappa_{0G}\exp[-(r/a)^2]. \quad \text{(S.6)}$$

The approximate basic reproductive number $R_{0c}(x_0, y_0)$ in Eq. S.4 depends on the position of the initial inoculum x0, y0. In order to obtain a single quantity for a particular spatial configuration of the host population, we average $R_{0c}(x_0, y_0)$ over all possible values of x_0, y_0 within the field:

$$\langle R_{0c}(x_0, y_0)\rangle_{x,y} = \int_0^{d_x} dx \int_0^{d_y} dy\, R_0'(x, y). \quad \text{(S.7)}$$

In the case of the Gaussian dispersal kernel the Eq. S.7 yields:

$$\langle R_{0c}(x_0, y_0)\rangle_{x_0,y_0} = \frac{d^2}{d_x d_y}\frac{\beta K}{\mu}\left(\sqrt{\frac{2}{\pi}}(\exp[-d_x^2/(2a^2)] - 1) + \frac{d_x}{a}\mathrm{erf}\left[\frac{d_x}{\sqrt{2}a}\right]\right) \times \quad \text{(S.8)}$$

$$\left(\sqrt{\frac{2}{\pi}}(\exp[-d_y^2/(2a^2)] - 1) + \frac{d_y}{a}\mathrm{erf}\left[\frac{d_y}{\sqrt{2}a}\right]\right). \quad \text{(S.9)}$$

In Figure S1, the approximate basic reproductive numbers $R_{0c}(x_0, y_0)$ calculated using Eq. S.5 (dotted curves), the spatially averaged $\langle R_{0c}(x_0, y_0)\rangle_{x_0,y_0}$ [Eq. S.8, dashed curve] and the exact basic reproductive number obtained by solving Eq. A.3 (solid curve) are plotted versus the field size d. The approximate $R_{0c}(x_0, y_0)$ is highest when the initial inoculum is introduced to the center of the field (upper dotted curve in Fig. S1) and is lower at the field border and in its corner (middle and lower dotted curves in Fig. S1). The spatial averaged $\langle R_{0c}(x_0, y_0)\rangle_{x_0,y_0}$ is reasonably close to the actual R_0 (cf. dashed and solid curves in Fig. S1), but it underestimates the actual R_0, because it neglects the contribution of the subsequent generations of infection. At $d \gg a$ the R_0 tends asymptotically to the maximal value of $R_{0c}(x_0, y_0)$, achieved at the field center $x = d/2, y = d/2$. The values of $R_{0c}(x_0, y_0)$ at the border and in the corner of the field also reach constant but considerably smaller values at $d \ll a$. This can be explained by the fact that when the size of the field increases, the surface-to-volume ratio of the square field decreases, meaning that the contribution of the hosts close to the field border to R_0 steadily decreases.

All the curves in Fig. S1 behave in the same way at small field sizes (i. e. when $d \ll a$): they increase quadratically with the field size d, according to

$$R_{0\mathrm{asympt}} = \frac{\beta K}{2\pi a^2 \mu} d^2. \quad \text{(S.10)}$$

Thus, the approximate expression for the basic reproductive number Eq. S.4 holds well in the two limiting cases: at small field sizes (i. e. when $d \ll a$) and at large field sizes (i. e. when $d \gg a$).

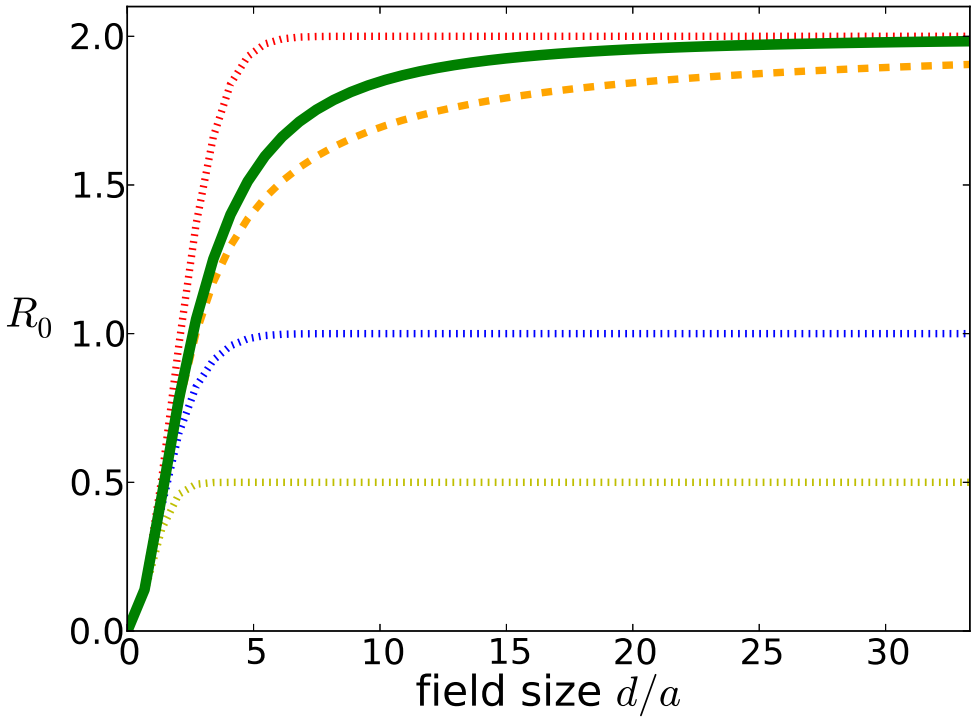

Figure S1: Basic reproductive number R_0 as a function of the field size d of the square two-dimensional field measured in units of the dispersal radius for the Gaussian dispersal kernel [Eq. S.6]. Solid curve shows the R_0 computed by solving the eigenvalue problem in Eq. S.3. Dotted curves represent the approximate $R_{0c}(x_0,\, y_0)$, according to Eq. S.5 with the initial inoculum located at the field center ($x_0 = y_0 = d/2$, upper curve), at the field border ($x_0 = d/2$, $y_0 = 0$, middle curve) and in the corner of the field ($x_0 = 0$, $y_0 = 0$, lower curve). The dashed curve shows the average $\langle R_{0c}(x_0,\, y_0)\rangle_{x_0,y_0}$ over the field, according to Eq. S.8. Model parameters: $\beta = 4$, $K = 1$, $\mu = 2$.

S.3. Estimation of the basic reproductive number as a function of the field size and shape

The basic reproductive number, R_0 can be determined as the dominant eigenvalue of the Fredholm equation Eq. S.3 We compute it as a function of the dimensions d_x and d_y of a rectangular field, which characterize its size and shape. To do this, we obtain numerical estimates for the dispersal kernel $\kappa(r)$ (Sec. S.3.1 and Sec. S.3.2) and the parameter combination $\beta K/\mu$ (Sec. S.3.3), which as we will show corresponds to the limit of R_0 at $d_x, d_y \to \infty$.

S.3.1. Fitting disease gradients

Disease gradients were measured in terms of both average number of lesions per leaf and disease severity in a large-scale experiment over three consecutive seasons (Sackett and Mundt, 2005*a*; Cowger et al., 2005). The datasets corresponding ot the average numbers of lesions per leaf in primary disease gradients were fitted using several different model functions (Sackett and Mundt, 2005*a*). Here, we also fitted the disease severity measurements corresponding to primary disease gradients (Fig. 2) for the two largest datasets (Hermiston 2002 and Madras 2002) of the experiments (Sackett and Mundt, 2005*a*; Cowger et al., 2005).

The following model functions are often used to fit the disease gradient data. Lambert kernel (Lambert et al., 1980)

$$y_{\mathrm{L}}(r) = y_0 \exp[-(r/a)^n], \tag{S.11}$$

which includes the special cases of the exponential (or Laplacian) kernel at $n = 1$ and the Gaussian kernel at $n = 2$. Power-law kernel (Gregory, 1968)

$$y_{\mathrm{PL}}(r) = y_0 r^{-b} \tag{S.12}$$

is used to describe disease gradients of pathogens with long-range dispersal. However, the function approaches infinity at the focus $r = 0$, which is unrealistic. For this reason a modified power-law kernel was introduced (Mundt and Leonard, 1985)

$$y_{\mathrm{PL1}}(r) = y_0 (r_0 + r)^{-b}. \tag{S.13}$$

It exhibits the same behavior as the power-law kernel in Eq. S.12 at large r, but the divergence is "softened" such that the function has a finite value at $r = 0$. In this study, we used a different form of the modified power-law kernel

$$y_{\mathrm{PL2}}(r) = y_0 \left(r_0^2 + r^2\right)^{-b/2} \tag{S.14}$$

that is very similar to Eq. S.13, but is more suitable for extensive numerical computations required for the solution of the eigenvalue problem in Eq. 6.

Figure 2 shows the primary disease gradients in terms of the disease severity for the two largest datasets obtained in (Cowger et al., 2005; Sackett and Mundt, 2005*a*): Hermiston 2002 (left panel) and Madras 2002 (right panel). Both of the datasets were fitted using the exponential kernel [Eq. S.11 with $n = 1$], Lambert kernel [Eq. S.11], modified power law 1 [Eq. S.13, fit not shown] and modified power law 2 [Eq. S.14]. The two modified power laws provided best fits with the modified power law 2 being slightly better. It is our kernel of choice, since it also allows for faster numerical

solutions of the eigenvalue problem in Eq. 6. We fix the parameter

The fit of the modified power-law function in Eq. S.14 to the disease gradient data shown in Fig. 2 yielded the following estimates for the parameter values:

$$\text{Hermiston 2002 downwind } b = 2.51 \pm 0.03,\ y_0 = 0.65 \pm 0.054; \tag{S.15}$$

$$\text{Madras 2002 downwind } b = 2.41 \pm 0.06, y_0 = 0.095 \pm 0.016. \tag{S.16}$$

Here, the uncertainties represent 95 % confidence intervals that were calculated from standard errors.

S.3.2. Definition and normalization of the dispersal kernel

We defined the dispersal kernel $\kappa(x, y, u, v)$ as a probability density function for an infectious spore to land at a distance r from its source (Nathan et al., 2012). The fact that a spore should eventually land somewhere is reflected in the condition to normalize the dispersal kernel:

$$\int_0^{2\pi} d\theta \int_0^{\infty} dr r \kappa(r, \theta) = 1. \tag{S.17}$$

Here, we transformed the dispersal kernel to polar coordinates using the relationships $x = r\cos\theta$, $y = r\sin\theta$. In the case of isotropic dispersal $\kappa(r, \theta) = \kappa(r)$, i. e. the dispersal kernel does not depend on the angle of dispersal θ. Then the normalization condition reads

$$2\pi \int_0^{\infty} dr r \kappa(r) = 1. \tag{S.18}$$

Next, we provide the normalization condition for the modified power-law function $Y_{\mathrm{PL2}}(r)$ [Eq. S.14] and for the Lambert function [Eq. S.11].

The dispersal kernel $\kappa(r)$ is assumed to be proportional to the disease gradient $y(r)$ (see Sec. 3.2). Therefore, the dispersal kernel should be given by the same function as the disease gradient

$$\kappa_{\mathrm{PL2}}(r) = \kappa_{0\mathrm{PL2}} \left(r_0^2 + r^2\right)^{-b/2}, \tag{S.19}$$

but with the different proportionality constant κ_0, which is obtained by substituting the Eq. S.19 into the normalization condition Eq. S.18:

$$\kappa_{0\mathrm{PL2}} = (b-2) r_0^{b-2}/(2\pi). \tag{S.20}$$

This expression is valid only if the integral in Eq. S.18 converges, which is the case at $b > 2$. In both datasets used here (Hermiston 2002 and Madras 2002 downwind) this condition is fulfilled for the values of b, corresponding to the best fit.

Similarly, the Lambert dispersal kernel has the form:

$$\kappa_{\mathrm{L}}(r) = \kappa_{0\mathrm{L}} \exp[-(r/a)^n], \tag{S.21}$$

where

$$\kappa_{0\mathrm{L}} = \frac{1}{\pi a^2 \Gamma\left(\frac{2+n}{n}\right)} \tag{S.22}$$

is determined from the normalization condition Eq. S.18.

We use the numerical values for the best-fit parameters Eq. S.15 and Eq. S.16 to obtain estimates for κ_0 using Eq. S.20:

$$\text{Hermiston 2002 downwind}: \ \kappa_0 = 0.071, \tag{S.23}$$

$$\text{Madras 2002 downwind}: \ \kappa_0 = 0.058. \tag{S.24}$$

Thus, our estimates for the dispersal kernels $\kappa(r)$ are given by the Eq. S.19 with the parameter values from Eq. S.15 and Eq. S.23 for Hermiston 2002 downwind; and from Eq. S.16 and Eq. S.24.

S.3.3. Estimation of the R_0 in the limit of a large field size

First, we consider the host population to be initially fully susceptible and have the leaf area index of K_0. Then, we introduce a localized unit of infected hosts (focus or source, hence the index "s") at a position x_s, y_s

$$H(x, y, t = 0) = K, \ I(x, y, t = 0) = I_{\mathrm{tot}0}\delta(x - x_s)\delta(y - y_s). \tag{S.25}$$

We are interested here only in the primary infections occuring due $I(x, y, t = 0)$, because the amount of disease due to the primary infection (or the primary disease gradient) is often measured in experiment (for example, (Sackett and Mundt, 2005*a*)). Hence, we derive the amount of infection produced after a single time step Δt from Eq. 2:

$$\left[I(x, y, t = \Delta t) - I(x, y, t = 0)\right] / \Delta t = \tag{S.26}$$

$$\beta \int_0^{d_x} du \int_0^{d_y} dv \kappa(x, y, u, v) I(u, v, t = 0) H(x, y, t = 0) - \mu I(x, y, t = 0) \tag{S.27}$$

By substituting Eq. S.25 in Eq. S.26 we obtain

$$\Delta I(x, y, t = \Delta t) = I_{\mathrm{tot}0}\Delta t \, K_{\Delta t}\beta\kappa(x, y, x_s, y_s), \tag{S.28}$$

where

$$\Delta I(x, y, t = \Delta t) = I(x, y, t = \Delta t) - I(x, y, t = 0) \tag{S.29}$$

represents the primary disease gradient from a localized point-like source. Further, we assume dispersal to be isotropic and set the coordinate of the focus to zero, i. e. $x_s = 0$. Then, the amount if infected host in the next time step and the dispersal function depend only on the distance $r = \sqrt{x^2 + y^2}$ from the focus, i. e. $I(x, y, t = \Delta t) = I(r, t = \Delta t)$, $\kappa(x, y, x_s, y_s) = \kappa(r)$. We can then re-write the Eq. S.28:

$$\Delta I(r, t = \Delta t) = I_{\mathrm{tot}0}\Delta t \, K_{\Delta t}\beta\kappa(r), \tag{S.30}$$

Next, we connect $\Delta I(x, y, t = \Delta t)$ with the whole-plant disease severity $y(r)$.

The quantity $I(r, t)$ in our model that represents the spatial density of the infected host tissue. In the case of wheat stripe rust it is the infected leaf area per unit land area (in analogy with the

"leaf area index" (LAI), we will call it the "infected leaf area index" (ILAI)). We express the disease severity as a ratio $y(r) = \mathcal{I}(r)/\mathcal{K}_{\Delta t}$, where $\mathcal{I}(r)$ is the total infected leaf area at a location r and $\mathcal{K}_{\Delta t}$ is the total leaf area at a location. By dividing both the numerator and the denominator of this expression by the unit land area Δs, we obtain $y(r) = \Delta I(r)/K_{\Delta t}$, where $\Delta I(r)$ is given by Eq. S.29, and $K_{\Delta t}$ is the total leaf area index. Therefore,

$$\Delta I(r,t) = \Delta t) = K_{\Delta t} y(r). \tag{S.31}$$

On the other hand, from Eq. S.30

$$\Delta I(r, t = \Delta t) = \beta K_{\Delta t} \Delta t I_{\text{tot}0} \kappa(r). \tag{S.32}$$

By equating Eq. S.31 and Eq. S.32 we obtain the relationship

$$\frac{\beta}{\mu} = \frac{1}{I_{\text{tot}0}} \frac{y(r)}{\kappa(r)}. \tag{S.33}$$

Here we assumed $\Delta t = 1/\mu$, which implies that the consecutive pathogen generations do not overlap (see the discussion in Sec. S.1). We multiply both sides of the Eq. S.33 by the leaf area index $K_{\Delta t}$ at time $t = \Delta t$ and obtain the expression for $R_{0\infty} = \beta K_{\Delta t}/\mu$

$$R_{0\infty} = \frac{K_{\Delta t}}{I_{\text{tot}0}} \frac{y_0}{\kappa_0}. \tag{S.34}$$

Here we used the fact that $\kappa(r)$ is proportional to $Y(r)$ and, therefore, their ratio equals to the ratio y_0/κ_0.

Now, we determine the intensity of the initial inoculum $I_{\text{tot}0}$ [Eq. S.25] from experimental parameters. The δ-functions in Eq. S.25 represent an infinitely narrow peak of a unit height. This is an idealized mathematical entity that can, however, be quite useful. It describes the actual situation well if the spatial scale of interest is much larger than the size of the focus. This was the case in the studies (Sackett and Mundt, 2005*a*; Cowger et al., 2005), where the focus (the area inoculated initially) was a square with the side $\Delta x_f = 1.52$ m, while the spatial scale over which the epidemic developed in the next generation was 50-80 m for the two largest datasets (Hermiston 2002 and Madras 2002 downwind).

$$\int_0^{\Delta x_f} dx \int_0^{\Delta x_f} dy I_{\text{tot}0} \delta(x - x_s)\delta(y - y_s) = I_{\text{tot}0} = \int_0^{\Delta x_f} dx \int_0^{\Delta x_f} dy I_0 = y_f K_0 \Delta {x_f}^2. \tag{S.35}$$

Here, y_0 is the disease severity at the focus caused by artificially inoculated spores (first generation) and K_0 is the leaf area index at the time of inoculation ("zeroth" generation). The Eq. S.35 says what the intensity of the initial inoculum should be if it was concentrated in a very small area such that the total amount of disease is the same as in the experiment.

$$I_{\text{tot}0} = y_f K_0 \Delta x_f^2. \tag{S.36}$$

After substituting Eq. S.36 into Eq. S.34 we obtain:

$$R_{0\infty} = \frac{K_{\Delta t}}{K_0} \frac{1}{y_f \Delta x_f^2} \frac{y_0}{\kappa_0}. \tag{S.37}$$

The expression in Eq. S.37 now consists of the parameters that are known from a typical disease gradient experiment.

We use the estimates we obtained above for the parameters y_0 [Eq. S.15 and Eq. S.16] and κ_0 [Eq. S.23 and Eq. S.24], also use the area of the focus $\Delta x_{\mathrm{f}}^2 = 1.52 \text{ m} \times 1.52 \text{ m} = 2.31 \text{ m}^2$ for both datasets and the values for the initial disease severity $y_f = 0.227$ (Hermiston 2002) and $y_f = 0.062$ (Madras 2002) (Cowger et al., 2005). We also assume that the leaf area index at the time of inoculation K_0 was two times smaller than its value at the time of disease gradient measurement, when the plants almost reached their maximum size, i. e. $K_{\Delta t} = 2K_0$. By substituting these values into Eq. S.37 we obtain the estimates for $R_{0\infty}$:

$$\text{Hermiston 2002 downwind } R_{0\infty} = 34.6 \pm 2.9; \tag{S.38}$$

$$\text{Madras 2002 downwind } R_{0\infty} = 22.9 \pm 3.8. \tag{S.39}$$

The uncertainties in the $R_{0\infty}$ estimates in Eq. S.38 and Eq. S.39 represent 95 % confidence intervals. Here, we only took into account errors in the parameter y_0 (see Eq. S.15 and Eq. S.16 above) and neglected errors in other parameters, because they are much smaller than errors in y_0.

Having obtained the numerical values for the parameter $R_{0\infty} = \beta K_{\Delta t}/\mu$ and the function $\kappa(r)$, we solved the eigenvalue problem in Eq. S.3 numerically for different values of d_x and d_y and determined the basic reproductive number R_0 as a function of the field size and shape. The results of this computation are shown in Fig. 3 and Fig. 4.

S.4. Susceptible-infected model with spatial spore dispersal

In this section we consider the model that takes into account spore dynamics explicitly. Our goal here is to describe the approximation that was used to obtain the simplified model Eqs. (1)-(2) that do not explicitly include spore dynamics. For the sake of brevity we consider the model in one-dimensional space, but it is straightforward to extend the consideration to two dimensions. The model of host-pathogen population dynamics reads

$$\frac{\partial H(x,t)}{\partial t} = r_H(K - H(x,t)) - \beta' \int_0^d \kappa(|s-x|)U(s,t)ds\, H(x,t), \tag{S.40}$$

$$\frac{\partial I(x,t)}{\partial t} = \beta' \int_0^d \kappa(|s-x|)U(s,t)ds\, H(x,t) - \mu I(x,t), \tag{S.41}$$

$$\frac{\partial U(x,t)}{\partial t} = \gamma I(x,t) - \mu' U(x,t), \tag{S.42}$$

where $H(x,t)$, $I(x,t)$ represent the areas covered by susceptible and infected host tissue, correspondingly, per unit area of the field; and $U(x,t)$ represents the number of spores per unit area of the field. Susceptible hosts $H(x,t)$ grow with the rate r_H. Their growth is limited by the "carrying capacity" K, implying limited space or nutrients. Furthermore, susceptible hosts $H(x,t)$ may be infected by the pathogen and transformed into infected hosts in the compartment $I(x,t)$ with the

transmission rate β'. The corresponding terms in Eqs. (S.40)-(S.41) are proportional to the amount of the available susceptible tissue $H(x,\, t)$ and to the amount of the infectious spores $U(x,\, t)$ at the location x. Infectious spores are produced at the rate γ and lost at the rate μ'.

Here, $\kappa(|s-x|)$ is the dispersal kernel that characterizes the probability of an infectious spore, produced at the location s to land at the location x. The integration is performed over all possible sources of spores within the field, i. e. over the whole extension of the field from 0 to d, where d is the size of the field. We assume that the dispersal kernel depends only on the distance $|s-x|$. The fact that the spore should land somewhere allows to normalize this function such that the integral of it over the whole space is unity:

$$\int_0^\infty \kappa(r)J(r)dr = 1, \tag{S.43}$$

where $J(r) = 1$ for the one-dimensional case considered here, and $J(r) = r$ for the two-dimensional case (in this case additional integration over the polar angle is required).

We assume that the characteristic time scale of spore dispersal is much shorter than the characteristic time scales associated with other stages of the pathogen life cycle. Then, the equation for spores is assumed to quickly assume the equilibrium state, with the left-hand side equal to zero and $U(x,\, t) = (\gamma/\mu')I(x,\, t)$. This means that the density of spores is proportional the density of the infectious host tissue. By substituting this expression into Eqs. (S.40)-(S.42), we reduce the model to just two Eqs. (1)-(2), where the transmission rate is a compound parameter: $\beta = \gamma\beta'/\mu'$.

S.5. Effect of the plot size on fungicide dose-response

In this section we present details on how we obtained the results described in Sec. 3.3 and in Fig. 5 of the main text. The data on disease severity of stripe rust versus the dose of epoxiconazole fungicide were taken from the Home-Grown Cereal Authority (HGCA) project report (Bounds et al., 2012). We chose epoxiconazole among several other fungicides considered in (Bounds et al., 2012), because it is an important and widely used fungicide for controlling stripe rust. Moreover, the dose-response curves for other fungicides are similar. Hence, we expect qualitatively similar outcomes.

We first estimate the fungicide dose-response parameters ε_{m} and D_{50}. To do this, we determine the relationship between the decrease in the transmission rate β and the decrease in the disease severity, y, defined as

$$y(t) = \frac{I(t) + R(t)}{I(t) + R(t) + H(t)}, \tag{S.44}$$

where $H(t)$, $I(t)$ and $R(t)$ are solutions of Eqs. (1)-(3). In the following, we consider the case when the threshold for epidemic development is exceeded, i. e. $R_0 > 1$.

Initially, the host density in the infected compartment grows exponentially

$$I = I_0 \exp\left[r(D)t\right], \tag{S.45}$$

where the growth rate, $r(D)$, depends on the fungicide dose D. $r(D)$ is related to other model parameters in the following manner

$$r(D) = \beta[1-\varepsilon(D)]K - \mu = \mu\left[R_0(D) - 1\right], \tag{S.46}$$

where

$$R_0(D) = R_0(D=0)\,[1-\varepsilon(D)] \tag{S.47}$$

and $\varepsilon(D)$ is given by Eq. 9 in the main text.

Next, we substitute the Eq. S.45 in Eq. 3 and perform integration with respect to time t, to obtain $I(t)+R(t) = I_0\,[(1+\mu/r(D))\,\exp\,[r(D)t] - \mu/r(D)]$. The assumption of exponential growth of $I_{\rm s}(t)$ implies in addition that $I(t)+R(t)+H(t) \approx K$. Consequently, using Eq. S.45, we obtain the expression for the disease severity, neglecting the dependence of the coefficient before the exponential function on the fungicide dose D:

$$y(t) = y_0 \exp\left[(R_0[1-\varepsilon(D)]-1)\,t\right], \tag{S.48}$$

where we neglected the term $I_0\mu/r(D)$, as it is much smaller than the exponentially growing term.

In contrast, over large times (but within a single growing season), disease severity approaches a constant value (Gilligan, 1990; Madden et al., 2006). For simplicity, we approximate the dependence of the disease severity on time using the logistic function

$$y(t) = \frac{1}{1+(1/y_0-1)\exp\left[(-R_0[1-\varepsilon(D)]-1)\,t\right]}, \tag{S.49}$$

which behaves as an exponential in Eq. S.48 during the initial phase and approaches unity over large times.

Further, we fit the expression for the disease severity in Eq. S.49 to the the empirical dose-response curve for epoxiconazole (triangles in Fig. 5(a)). To do this, we set the time of fungicide application to zero ($t_0 = 0$), use $\kappa = 1$, set $t_1 \approx 32$ days (Bounds et al., 2012), and $\mu = 0.033$ day^{-1} (Sache and Vallavieille-Pope, 1993). We also use the value of the basic reproductive number in the absence of fungicides $R_0(D=0,\,S=60\ \mathrm{m}^2) = 12.6$. We obtained this estimate using the Hermiston 2002 disease gradient dataset (Sackett and Mundt, 2005*a*; Cowger et al., 2005) for a square field with the area of ≈ 60 m^2, which is the field size used in the field experiments where fungicide dose-response curves were measured (Bounds et al., 2012). We consider the initial severity, y_0, and the dose-response parameters, $\varepsilon_{\rm m}$ and D_{50}, as fitting parameters. As a result, we obtain the best-fit estimates:

$$\varepsilon_{\rm m} = 0.290 \pm 0.009,\ D_{50} = 0.050 \pm 0.013,\ y_0 = (2.9 \pm 0.025)\times 10^{-8}. \tag{S.50}$$

The uncertainties in Eq. S.50 represent the 95 % confidence intervals.

We substitute the best-fit values of $\varepsilon_{\rm m}$ and D_{50} from Eq. S.50 in Eq. S.47, and estimate the dependence of the basic reproductive number on the fungicide dose at the field size that was used in the din Fig. 5(b) in the main text). Next, assuming that the fungicide and the field size affect the basic reproductive number as independent factors, i. e. multiplicatively, we determine the dependence of the basic reproductive number on the fungicide dose at a 50 % larger field size of $S = 90$ m^2, linear extension $d = 9.5$ m (dashed red curve in Fig. 3(b)). We do this using the same values of the dose-response parameters $\varepsilon_{\rm m}$ and D_{50} (Eq. S.50), but a different value of R_0 in the absence of fungicides, $R_0(D=0,\,d=9.5\ \mathrm{m}) = 16$, that we estimated from the Hermiston 2002 disease gradient dataset (see solid red curve in Fig. 3). Finally, we compute the dependence of the disease severity on the fungicide dose for this larger field size, by substituting Eq. S.50 and $R_0(D=0,\,d=9.5\ \mathrm{m}) = 16$ in

Eq. A.50. The result is shown as a dashed red curve in Fig. 5(a).

References

Press, W. H., S. A. Teukolsky, W. T. Vetterling, and B. P. Flannery, 1992. Chapter 18. Integral Equations and Inverse Theory. Page 788 *in* Numerical Recipes in C. Cambridge University Press, Cambridge.

Anderson, R. M., and R. M. May. 1986. The invasion, persistence and spread of infectious diseases within animal and plant communities. Philosophical transactions of the Royal Society of London. Series B, Biological sciences **314**:533–70.

Diekmann, O., J. A. P. Heesterbeek, and J. A. J. Metz. 1990. On the definition and the computation of the basic reproduction ratio R0 in models for infectious diseases in heterogeneous populations. Journal of Mathematical Biology **28**:365–382.

Sackett, K. E., and C. C. Mundt. 2005*a*. Primary disease gradients of wheat stripe rust in large field plots. Phytopathology **95**:983–91.

Cowger, C., L. D. Wallace, and C. C. Mundt. 2005. Velocity of spread of wheat stripe rust epidemics. Phytopathology **95**:972–82.

Lambert, D. H., R. L. Villareal, D. R. Mackenzie, and T. P. Agri. 1980. A General Model for Gradient Analysis. Phytopathol. Z. **154**:150–155.

Gregory, P. 1968. Interpreting plant disease dispersal gradients. Annual Review of Phytopathology **6**:189.

Mundt, C., and K. Leonard. 1985. A modification of Gregory's model for describing plant disease gradients. Phytopathology **75**:930.

Nathan, R., E. Klein, J. J. Robledo-Arnuncio, and E. Revilla, 2012. Dispersal kernels: review. Chapter 15, page 187 *in* J. Clobert, M. Baguette, T. G. Benton, and J. M. Bullock, editors. Dispersal ecology and evolution. Oxford Univ. Press.

Bounds, P., J. Blake, B. Fraaije, D. Parsons, S. Knight, F. Burnett, J. Spink, and J. McVittee. 2012. Fungicide performance on winter wheat. Home-Grown Cereals Authority, UK, Project Report 488 .

Gilligan, C. 1990. Comparison of disease progress curves. New Phytologist **115**:223.

Madden, L., G. Hughes, and F. van den Bosch. 2006. The Study of Plant Disease Epidemics. APS Press, St. Paul, Minnesota USA.

Sache, I., and C. Vallavieille-Pope. 1993. Comparison of the wheat brown and yellow rusts for monocyclic sporulation and infection processes, and their polycyclic consequences. Journal of phytopathology **138**:55–65.